Connexin hemichannels contribute to spontaneous electrical activity in the human fetal cortex

Anna R. Moore, Wen-Liang Zhou, Carissa L. Sirois, Glenn S. Belinsky, Nada Zecevic, and Srdjan D. Antic[1]

Department of Neuroscience, University of Connecticut Health Center, Farmington, CT 06030

Edited by Pasko Rakic, Yale University, New Haven, CT, and approved August 1, 2014 (received for review April 7, 2014)

Before the human cortex is able to process sensory information, young postmitotic neurons must maintain occasional bursts of action-potential firing to attract and keep synaptic contacts, to drive gene expression, and to transition to mature membrane properties. Before birth, human subplate (SP) neurons are spontaneously active, displaying bursts of electrical activity (plateau depolarizations with action potentials). Using whole-cell recordings in acute cortical slices, we investigated the source of this early activity. The spontaneous depolarizations in human SP neurons at midgestation (17–23 gestational weeks) were not completely eliminated by tetrodotoxin—a drug that blocks action potential firing and network activity—or by antagonists of glutamatergic, GABAergic, or glycinergic synaptic transmission. We then turned our focus away from standard chemical synapses to connexin-based gap junctions and hemichannels. PCR and immunohistochemical analysis identified the presence of connexins (Cx26/Cx32/Cx36) in the human fetal cortex. However, the connexin-positive cells were not found in clusters but, rather, were dispersed in the SP zone. Also, gap junction-permeable dyes did not diffuse to neighboring cells, suggesting that SP neurons were not strongly coupled to other cells at this age. Application of the gap junction and hemichannel inhibitors octanol, flufenamic acid, and carbenoxolone significantly blocked spontaneous activity. The putative hemichannel antagonist lanthanum alone was a potent inhibitor of the spontaneous activity. Together, these data suggest that connexin hemichannels contribute to spontaneous depolarizations in the human fetal cortex during the second trimester of gestation.

UP states | brain development | glutamate | GABA | preterm infants

In the adult brain, neuronal network activity is essentially driven by chemical synapses (1–3), whereas in the developing brain, neuronal activity is largely independent of sensory inputs (4–6). Membrane depolarizations during the earliest stages of brain development play an important role in the transition between the immature and mature signaling properties of neurons, as well as in shaping the mature functional neuronal network (7–12). Recent studies performed in the rodent model of cortical development have implicated subplate (SP) neurons as key regulators of early electrical activity and network oscillations (13, 14). Their essential role in the establishment of thalamocortical connections and cortical columns (15–18), extensive connectivity within the early synaptic network (19–21), and dense gap junction coupling (22, 23), as well as the abundant innervation by neuromodulatory transmitter systems (24, 25), put SP neurons in an ideal position to synchronize cortical activity during early development. Disruptions to the SP zone during development have been implicated in several major neurological disorders including schizophrenia, cerebral palsy, and autism (26, 27).

Most of the physiological studies on SP neurons have been performed in the first postnatal week of rodent development [postnatal day 0 (P0) to P4], a time that corresponds more closely to the last (third) trimester of human gestation (28). Little is known about human SP neuron physiology in the first two trimesters, when massive proliferation, neuron migration and the initial stage of network formation are occurring in the human cerebral cortex (29, 30). General principles arising from the rodent model of cortical development should be tested in human neurons whenever possible, because it is well established in neurobiology that similar activity patterns can be produced by different sets of underlying conductances (31).

Because of ethical and technical limitations associated with experimentation on human materials, there is a profound lack of information about physical, chemical, and biological agents that affect spontaneous electrical activity in human fetal cortex. Using acute brain slices obtained from postmortem human fetal tissue [17–23 gestational weeks (gw)], we analyzed the physiological effects of channel and receptor antagonists on SP neuron activity. We found that spontaneous bioelectric activity of human SP neurons is moderately influenced by drugs that block neuronal network activity and synaptic transmission and more strongly by drugs that interfere with the activity of connexin (Cx) pores. Several lines of our experimental data point to Cx hemichannels as significant contributors to spontaneous membrane depolarizations in human fetal cortex during the second trimester of gestation.

Results

We performed whole-cell recordings from SP neurons in acute fetal cortical slices to identify membrane conductances that support spontaneous electrical activity during the second trimester of gestation (17–23 gw). Anatomical and electrophysiological criteria for identification of SP neurons were previously established in animal and human research (32–34). SP neurons have greater cell diameters than the postmitotic neurons migrating through the SP zone (Fig. 1 *A1*) (see also ref. 34, figure 1), and the shape of the SP neuron soma is more elongated (Fig. 1 *A2*)

Significance

Young neurons require occasional bursts of action-potential firing to maintain intracellular processes, to drive gene expression, to indicate their presence in a new location, and to attract and keep synaptic contacts. While in the adult cortex electrical activity is driven by synaptic inputs, during early cortical development these synaptic inputs are largely absent. In the absence of synaptic connections and sensory experience, human neurons use an energetically favorable membrane mechanism for generating and maintaining electrical activity: connexin hemichannels. The spontaneous flickering of connexin hemichannels produces depolarizing events (often crowned with bursts of action potentials) to help establish early electrical communication in young subplate neurons. This type of activity dominates the human cortical wall 5 months before birth.

Author contributions: A.R.M., N.Z., and S.D.A. designed research; A.R.M., W.-L.Z., C.L.S., G.S.B., and S.D.A. performed research; A.R.M. and S.D.A. analyzed data; and A.R.M., N.Z., and S.D.A. wrote the paper.

The authors declare no conflict of interest.

This article is a PNAS Direct Submission.

[1]To whom correspondence should be addressed. Email: antic@neuron.uchc.edu.

This article contains supporting information online at www.pnas.org/lookup/suppl/doi:10.1073/pnas.1405253111/-/DCSupplemental.

compared with other cells in the same zone. Unlike migrating neurons, the SP neurons have long axonal processes (Fig. 1*B*). If the peak sodium current was >700 pA (voltage clamp) and the depolarizing current injections (current clamp) triggered repetitive firing of full-sized action potentials (APs), the cell was identified as an SP neuron (Fig. 1 *C*, *Inset*). Note that young neurons migrating through the SP zone do not exhibit full-size repetitive AP firing (33, 34). Once an SP neuron was identified, we proceeded to monitor spontaneous electrical activity with a drug-testing paradigm ($n = 126$ neurons; $n = 12$ human subjects; Table 1).

Extracellular Ca^{2+} Influences Spontaneous Electrical Activity. Human fetal SP neurons generate spontaneous electrical activity in vitro (Fig. 1*C*). To test whether spontaneous activity of human SP neurons changes as the fetus develops, the SP neurons were separated into three age groups (19–20, 21, and 22–23 gw) and compared in respect to four parameters of spontaneous activity: (*i*) event count; (*ii*) instantaneous frequency; (*iii*) peak amplitude; and (*iv*) surface area. We found that the number of depolarizing events grew gradually from 19 to 23 gw (Fig. S1*A*). We also found a significant change in the instantaneous frequency (or interevent interval frequency) between 19–20 and 21 gw (Fig. S1*B*). However, the peak amplitude of events and total surface area did not show any significant increase over the gestational ages observed (Fig. S1 *C* and *D*). Overall, although the change in activity levels across the examined gestational ages is relatively weak, the data do suggest a subtle increase in spontaneous electrical activity during the 5 wk examined in this study (19–23 gw).

The most prominent feature of the spontaneous electrical activity in human fetal SP neurons is the occurrence of prolonged silent periods (Fig. 1*C*). Periods of sustained depolarizations and AP firing ("UP states") are interrupted with long periods of quiescence (ref. 34, figure 2), resembling "tracé discontinu" in electroencephalogram recordings from preterm infants (35). Quite often these silent periods can last for several seconds to minutes (34), making the interpretation of pharmacological experiments difficult to achieve. Namely, the appearance of a prolonged silent period in either control or test (drug) condition would strongly bias the quantitative measurements of neuronal activity (*Methods*). We sought an experimental approach that would increase the incidence of SP "UP states" and thus reduce the impact of silent periods. It has been previously shown that lowering Ca^{2+} in the artificial cerebrospinal fluid (ACSF) improves spontaneous neuronal activity in vitro (36, 37).

In the first series of experiments, we established that lowering the extracellular calcium concentration from 2 to 1.2 mM significantly increased the spontaneous electrical activity of SP neurons ($n = 46$) (Fig. 1*C Lower*). Perfusion of brain slices with 1.2 mM $[Ca^{2+}]_o$ markedly increased both the frequency and duration of SP UP states (sustained depolarizations accompanied by AP firing). An all-points histogram revealed important differences between 2 mM $[Ca^{2+}]_o$ ACSF (Fig. 1*D*, white) and 1.2 mM $[Ca^{2+}]o$ ACSF (gray), especially at more depolarized potentials (≥45 mV). When bathed in 1.2 mM Ca^{2+} ACSF, SP neurons spent significantly more time at depolarizing potentials (45 mV and greater) compared with 2 mM $[Ca^{2+}]$ ACSF (Fig. 1 *D*, *Inset*; compare white and gray contours; $P < 0.001$; $n = 46$).

Altering the extracellular calcium concentration from 2 to 1.2 mM did not significantly change the total number of depolarizing events (56.3 ± 9.6 s vs. 72.9 ± 9.7 s; mean ± SEM, $P = 0.08$, $n = 46$; Fig. 1 *E*, *Left Upper*). However, lowering the Ca^{2+} concentration significantly increased the average peak amplitude of sustained depolarizations (7.3 ± 3 mV vs. 13.8 ± 1.5 mV; $P < 0.05$; Fig. 1 *E*, *Right Upper*), the duration of events (41 ± 7 s vs.

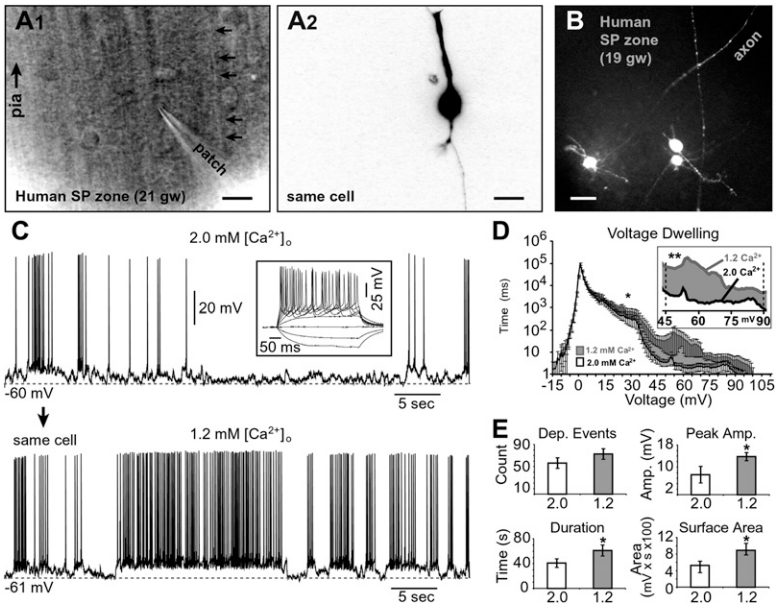

Fig. 1. Extracellular calcium concentration affects spontaneous activity of SP neurons. (*A1*) Surface of human fetal brain slice: differential interference contrast video-microscopy. Trajectory of one radial fiber is denoted by five arrows. (Scale bar, 10 μm.) (*A2*) Same cell shown in fluorescence channel. (*B*) Multiple processes emerge from human SP neurons. (Scale bar, 25 μm.) (*C*) Effects of lowering the extracellular calcium concentration $[Ca^{2+}]_o$ from 2.0 to 1.2 mM in the same cell ($n = 46$). In this and all subsequent figures, V_R denotes membrane potential at the beginning of the sweep, attained by a fixed holding current in the range from −3 to −22 pA. (*Inset*) Repetitive AP firing in response to a series of injected current pulses used to identify an SP neuron. (*D*) All-points histogram illustrating the average amount of time cells ($n = 46$) spent at a particular voltage (voltage dwelling) in 2.0 mM (white) vs. 1.2 mM (gray) $[Ca^{2+}]$. More time is spent at higher voltages if extracellular $[Ca^{2+}]$ were 1.2 mM. Error bars are SEM. Asterisk indicates significant difference between two conditions across entire voltage range. (*Inset*) Voltage range of 45–90 mV highlighting a highly significant difference between 2.0 and 1.2 mM. (*E*) Average number of depolarizing events, average peak amplitude (Amp.) of depolarizing (Dep.) events, total event duration (sum of all depolarizing events), and total surface area in 2.0 mM (white) and 1.2 mM (gray) $[Ca^{2+}]_o$. $^*P < 0.05$; $^{**}P < 0.01$.

Table 1. List of cases including age, sex, and total number of cells recorded in each case

Case no.	Age, gw	Sex	Cells
1	21	Female	27
2	21	Female	6
3	19	Unknown	7
4	22	Male	7
5	19	Female	14
6	19	Female	16
7	23	Female	14
8	23	Unknown	8
9	21	Male	3
10	21	Male	16
11	20	Female	7
12	17	Male	1

61.3 ± 8.9 s; $P < 0.05$; $n = 46$; Fig. 1 *E*, *Left Lower*), and total surface area (525.3 ± 106.3 mV·s vs. 890.1 ± 172.5 mV·s; $P < 0.05$; Fig. 1 *E*, *Right Lower*). These data demonstrate that lowering the extracellular Ca^{2+} concentration $[Ca^{2+}]_o$ from 2 to 1.2 mM resulted in a marked shortening of silent periods and more spontaneous electrical activity overall (Fig. 1). All subsequent experiments/recordings (control and test) were carried out in ACSF containing 1.2 mM $[Ca^{2+}]$.

Spontaneous Depolarizations Following Network Activity Blockade. Spontaneous network activity in developing circuits (37–43) generally comprises AP-mediated release of neurotransmitters and neuromodulators (44). To determine whether spontaneous electrical activity in human SP neurons at midgestation (17–23 gw) was also driven by AP-mediated release of neurotransmitters, we blocked AP initiation with bath application of tetrodotoxin (TTX; 1 μM).

Spontaneous (unprovoked) electrical activity was recorded before and after bath application of 1 μM TTX (Fig. 2*A*). A set of depolarizing currents was injected into the SP neuron to test the efficacy of TTX treatment (Fig. 2 *A*, *Insets*). The total number of spontaneous depolarizing events per standard recording time (5 min) in the presence of TTX (Fig. 2*B*, Dep. Events) was not statistically different from that measured in the same neuron before drug application ($P = 0.9$; $n = 16$). In the presence of TTX, the average peak amplitude of depolarizing events was significantly reduced from 20.9 ± 2.4 mV to 9.7 ± 1 mV ($P < 0.001$; Fig. 2*B*, Peak Amp.). The mean duration of all depolarizing events was reduced from 81.8 ± 15.8 s in control to 38.7 ± 12.3 s ($P = 0.07$), and the total surface area of events from 1,287.1 ± 345.7 mV·s in control vs. 481.3 ± 163.1 mV·s ($P = 0.06$) in TTX (Fig. 2*B*). Although sodium currents and AP firing were effectively blocked in our experiments (Fig. 2 *A*, *Insets*), many depolarizing events remained (Fig. 2 *A*, *Lower*). These data indicate that during the second trimester of gestation, spontaneous depolarizations occur in human SP neurons unrelated to AP firing in the surrounding neuronal networks.

Contribution of Chemical Synapses. In the next series of experiments we studied how antagonists of glutamatergic, GABAergic, and glycinergic synaptic transmission affect spontaneous activity. Blockade of AMPA/kainate receptors with 6,7-dinitroquinoxaline-2,3(1H,4H)-dione (DNQX; 20 μM) had a weak effect on the spontaneously occurring depolarizing events in the majority of SP neurons tested (Fig. 3*A*). In this experimental group, DNQX treatments did not produce a statistically significant change ($P > 0.05$; $n = 16$), in respect to five electrophysiological parameters, including: (*i*) the total number of depolarizing events (Fig. 3*E*); (*ii*) the average peak amplitude of depolarizing events; (*iii*) duration of individual events; (*iv*) total surface area; and (*v*) instantaneous frequency of spontaneously occurring depolarizing events (Fig. 3*E*). Similarly, blockade of GABA receptors with bicuculline (20 μM, $n = 15$; Fig. 3*B*) or blockade of glycinergic receptors with strychnine (20 μM, $n = 6$; Fig. 3*C*) did not produce a statistically significant effect on any of the five electrophysiological parameters (Fig. 3*E*). A combined blockade of AMPA/kainate, NMDA, GABA, and glycine receptors notably reduced the incidence and amplitude of spontaneously occurring depolarizing potentials in some cells (Fig. S2), but changes were not statistically significant when analyzed across the entire group ($n = 6$). Addition of TTX to the mixture of synaptic blockers [20 μM DNQX, 20 μM DL-2-amino-5-phosphonovaleric acid (APV), 20 μM bicuculline, 20 μM strychnine, and 1 μM TTX] also failed to significantly alter the parameters of spontaneous electrical activity, aside from the inhibition of AP firing (Fig. 3 *D*, *Right*).

It is important to emphasize that, in some cells, we occasionally observed suppression of spontaneous electrical activity in response to synaptic blockers. Because the five electrophysiological parameters used in the analysis did not reflect those changes (Fig. 3*E*), we decided to plot raw data points in a histogram. For example, an all-points histogram averaged across 16 cells shows that blocking of AMPA receptor currents with DNQX reduced the amount of time human SP neurons spent at higher voltages (Fig. 3*F*). If we omit the data points more negative than 30 mV ($P < 0.05$; $n = 16$), we see a significant difference between the cells' responses after treatment with DNQX. If all voltages are included (−10 to +100 mV), the difference between control (light gray) and DNQX-treated (dark gray) is not significant (Fig. 3*F*; $P > 0.05$; $n = 16$). This result is consistent with the larger error bars and lack of significance in the analysis of the five electrophysiological parameters (Fig. 3*E*). Similarly, an all-points histogram for the mixture of synaptic blockers and TTX (Syn. Block + TTX) was statistically significant if we analyzed voltages above +15 mV ($P < 0.05$) and was not statistically different from the control data if all voltages, −10 to +100, were included ($P > 0.05$ $n = 4$; Fig. 3*G*). One cell showed a strong

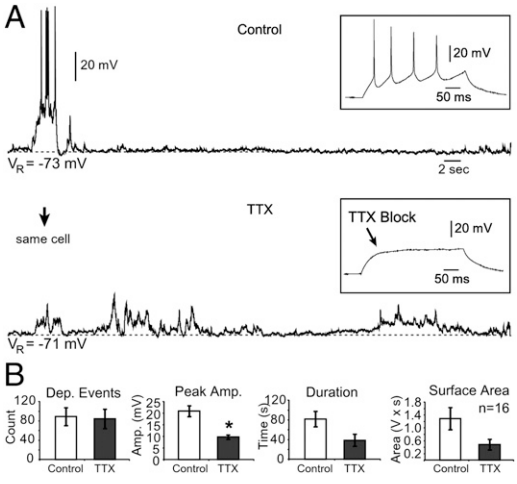

Fig. 2. Effects of AP blockade on the spontaneous electrical activity of human SP neurons. (*A*) Bath application of TTX (1 μM) blocks AP firing and reduces the duration and amplitude of depolarizing plateau potentials, but does not completely silence bioelectrical activity. (*Upper Inset*) Repetitive AP firing following an injection of depolarizing current. (*Lower Inset*) AP block during bath application of TTX. Dashed horizontal line, baseline membrane potential. (*B*) Quantification of the effects of TTX. Application of TTX (gray) does not reduce the number of depolarizing (Dep.) events, duration, and total surface area, but significantly reduces the peak amplitude (Amp.) compared with control (white). *$P < 0.05$.

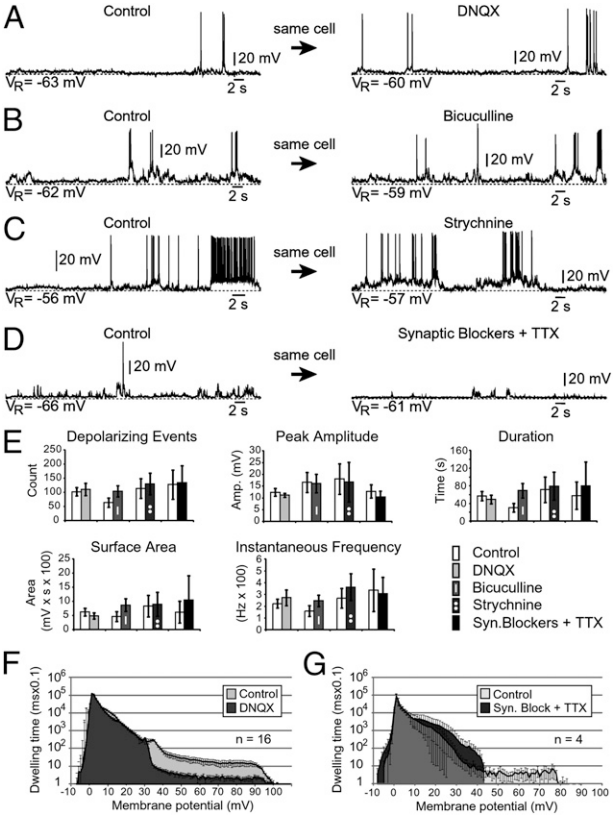

Fig. 3. Block of chemical synapses. (*A–D*) Spontaneous electrical activity in human SP neurons during application of DNQX (20 μM; *A*), bicuculline (20 μM; *B*), strychnine (20 μM; *C*), and synaptic block containing DNQX, APV, bicuculline, and strychnine (20 μM; *D*) in combination with TTX (1 μM). Dashed lines, baseline membrane potential. (*E*) Spontaneous activity in SP neurons before (white) and after (shaded) drug application was analyzed in respect to number of depolarizing events, peak amplitude, duration, surface area, and instantaneous frequency of depolarizing events. Statistically significant differences were not detected. (*F*) Averaged all-points histogram ($n = 16$ cells) before and after application of DNQX (20 μM). (*G*) Averaged all-points histogram ($n = 4$ cells) before and after application of synaptic block containing DNQX, APV, bicuculline, and strychnine (20 μM) in combination with TTX (1 μM). Statistically significant differences were not detected if the entire range of voltages (from −10 to +100 mV) was included in the *t* test.

decline in electrical activity in response to Syn. Block + TTX (Fig. 4*A*). Although it is possible that a greater number of cells examined would produce a statistically significant differences between control and test recordings in Fig. 3, our data highlight that, following a block of network AP firing combined with a block of glutamatergic, GABAergic, and glycinergic synaptic transmissions, the small spontaneous membrane depolarizations remained (Figs. 2*A* and 3*D*; Fig. 4*B*, rectangles). Together, these pharmacological data suggest that during the earliest stages of human cortical development, when the cortical plate (CP) has just begun to form, spontaneous depolarizations in SP neurons are not entirely dependent on AP firing in neuronal networks or synaptic inputs (glutamatergic, GABAergic, or glycinergic) within the cortical wall. Because of the weak effect on spontaneous activity observed in SP neurons following application of select synaptic blockers, in the next series of experiments, we focused our attention on the possible presence of functional gap junctions in human fetal brain.

Cx in the Human Fetal Cortex. Gap junctions and hemichannels have been broadly implicated in the control of embryonic patterning of the neocortex, including neuronal proliferation, maturation, and differentiation (45, 46). Gap junctions contribute to the generation of cortical circuits by mediating oscillatory patterns of electrical activity in the neonatal mouse cerebral cortex (7, 22, 47) and are an important means of intracellular communication at this age (46, 48). We therefore hypothesized that gap junctions may contribute to the generation of spontaneous membrane depolarizations observed in human SP neurons during the second trimester of gestation. To test this hypothesis, we first evaluated the expression of several Cx in the human fetal cortex at 17 and 19 gw. Isolated human fetal cortex or specific isolated brain regions containing the ganglionic eminence (GE), cortical subventricular zone (SVZ), or CP were analyzed by PCR. We found Cx26 mRNA expression at 17 and 19 gw, whereas Cx36 mRNA expression was only present at 19 gw (Fig. 5*A*). In addition, Cx43 mRNA expression was only detected in the GE at 17 gw (Fig. 5*A*). We did not detect Cx30, Cx31, or Cx32 mRNA expressions in either gestational age, whereas pannexin-1 was present in GE only (Fig. 5*A*). In the next set of experiments the expression of Cx32 was tested on fresh samples obtained at 17, 18, and 20 gw and cultured cells from a 22-gw human fetal brain (Fig. S3*B*). At all ages tested, we again did not detect any forms of Cx32 (variants 1 and 2) in these samples (Fig. S3*B*). Pannexin-1 was present in 17 and 18 gw, as well as in the commercial sample of the total human fetal brain RNA (Fig. S3*B*).

Using commercially available antibodies, we tested the presence of Cx32, Cx26, Cx36, and Cx43 protein in the human fetal cortex. Cx32 labeling was observed in individual cells of the SP zone during gw 20–22 (Fig. 5*B*, red). Labeling was sparse, appearing in only a small fraction of cells at a nominal density of one to five cells per visual field (210 by 210 μm) (Fig. 5*C*, arrowheads). The Cx32-positive cells (Fig. 5*C*, red) were large and colabeled with βIII-tubulin (green) and had the morphological appearance of SP neurons being either pyramidal-like with apical processes extending perpendicularly (Fig. 5*D*) or

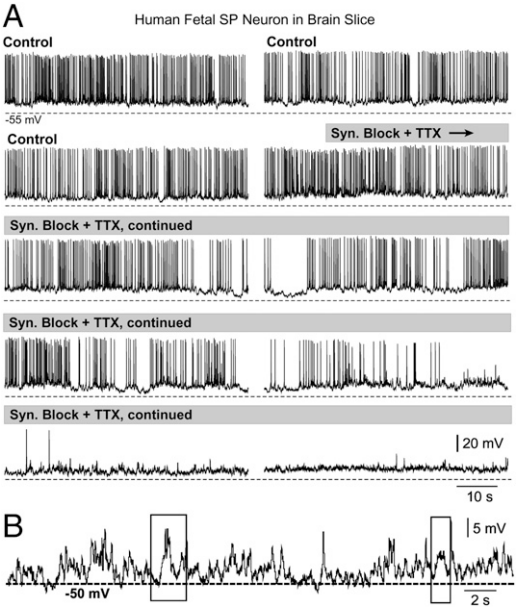

Fig. 4. Residual depolarizations. (*A*) Bath application of synaptic blockers [DNQX, APV, bicuculline, and strychnine (20 μM each)] in combination with TTX (1 μM) does not completely silence membrane depolarizations. The time course of drug perfusion is marked by gray rectangles. Dashed line below traces represents −55 mV. (*B*) Enlargement of one section of the bottom trace shown in *A*. Rectangles mark depolarizing events (~5 mV) that lasted >500 ms.

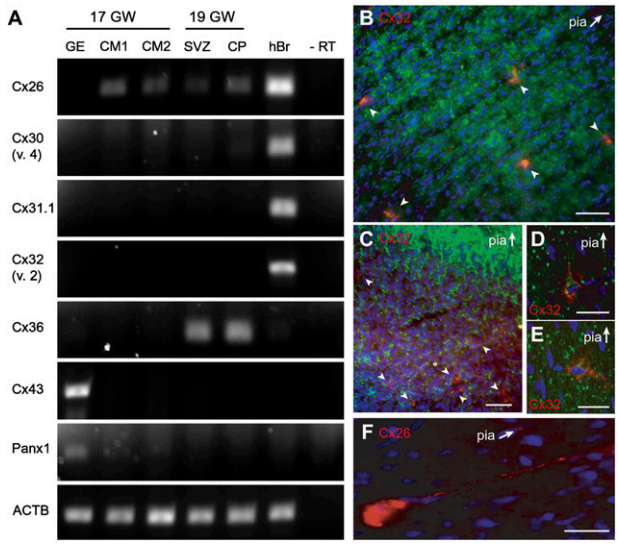

Fig. 5. Cx26 and Cx32 expression in the human cerebral cortex during the second trimester of gestation. (*A*) Human Cx mRNA expression measured by PCR from human fetal forebrain at 17 and 19 gw and compared with human adult brain (hBr) as a positive control. CM, cortical mantle. (*B*) Cx32 (red) staining was localized in the SP zone, but absent in the CP during the second trimester (βIII-tubulin, green; Hoechst, blue). (Scale bar, 50 μm.) (*C*) Cx32 (red) labeling in the *SP* zone is sparse and only present in a small number of cells (arrowheads). (Scale bar, 50 μm.) (*D* and *E*) Higher magnification of Cx32-positive cells in the *SP* revealed "vertical pyramidal" (*D*) and "horizontal pyramidal" (*E*) cells. (*F*) Cx26 (red) detected in the cell body and neuronal processes. [Scale bars (*D*–*F*), 20 μm.] Arrows point toward the pial surface. *B*–*F*, ages 20–22 gw.

horizontally (in parallel) to the pial surface (Fig. 5*E*) (32). Expression of Cx32 was found on isolated cells and not in clusters or groups of cells, suggesting that these Cx may be forming hemichannels and not gap junctions with other cells or processes. A similar expression pattern within the SP zone was found with Cx26; however, in addition to cell bodies, the Cx26 immunoreactivity also appeared in neuronal processes (Fig. 5*F*, red). We found no expression of Cx43 in the SP zone of the developing human cerebral cortex consistent with the PCR data (Fig. 5*A*). Immunolabeling of Cx36 in brain sections harvested from a 23-gw fetus revealed an abundance of Cx36-positive cells in the SP zone (Fig. 6 *A* and *B*) scattered on the background of GABA-positive radial fibers (Fig. 6 *B* and *C*). Approximately 50% of the cells in the human SP zones were Cx36-negative. The majority of the Cx36-negative cells appeared in clusters comprising three or four members (Fig. 6 *C2*, arrows), suggesting young postmitotic neurons migrating through the intermediate zone and SP zone. Together these results suggest that the distribution of Cx is spatially and temporally regulated in the human fetal telencephalon during the second trimester of gestation.

Gap Junctions. We next sought to determine whether gap junction signaling affects electrical activity of human SP neurons. A mixture of nonselective gap junction blockers—octanol (OCT; 1 mM), carbenoxolone (CBX; 100 μM), and flufenamic acid (FFA; 100 μM)—completely abolished AP firing in three cells and strongly reduced the number of depolarizations in another three cells (Fig. 7*A*). The mixture of Cx blockers (OCT+CBX+FFA) significantly reduced three of four electrophysiological parameters of spontaneous electrical activity ($n = 6$). A statistically significant reduction was detected between control conditions and in the presence of Cx blockers mixture (OCT+CBX+FFA) in the following: number of depolarizing events, 156.7 ± 31.8 vs. 26.5 ± 10.1, $P < 0.01$; duration of depolarizing events, 79.8 ± 47.8 s vs. 4.4 ± 1.6 s, $P < 0.01$; and total surface area, 1,280.2 ± 535.5 mV·s vs. 44.2 ± 0.2 mV·s; $P < 0.01$; Fig. 7*B*). However, peak amplitude of depolarizing events: 21 ± 3.2 mV vs. 12.4 ± 2.5 mV was not statistically different between Control and OCT+CBX+FFA condition ($P = 0.07$), largely due to sporadic AP firing (Fig. 7*A*).

Bath application of OCT alone (1 mM) caused a profound block of spontaneous electrical activity in three of five cells, whereas in the remaining two cells, the activity was markedly reduced (Fig. S4). Group data analysis ($n = 5$) found that application of OCT alone caused a statistically significant reduction in the number of depolarizing events (control: 53.8 ± 10.6; OCT: 16.3 ± 6.6; $P < 0.05$), duration of depolarizing events (control: 79.9 ± 47.8 s; OCT: 1.8 ± 0.9 s; $P < 0.05$), and total event surface area (control: 1,053.1 ± 640.6 mV·s; OCT: 12.1 ± 5.7 mV·s; $P < 0.05$). However, OCT did not significantly reduce the peak amplitude of spontaneous events (control: 24.4 ± 6.2 mV; OCT: 13.7 ± 3.8 mV; $P > 0.05$).

Cx Hemichannels. To determine whether the spontaneous electrical activity was regulated specifically via Cx hemichannels as opposed to gap junctions, we applied lanthanum (La^{3+}), a Cx hemichannel blocker that does not affect gap junctions and pannexin hemichannels when applied extracellularly at 50–200 μM (49–51). Bath application of La^{3+} (100 μM) strongly inhibited spontaneous electrical activity of human SP neurons (Fig. 8*A*; $n = 6$), with significant effects on the number of events (control, 138.8 ± 30.9; La^{3+}, 17.3 ± 5.7; $P < 0.01$), duration (control, 86.3 ± 11.3; La^{3+}, 7.8 ± 1.6 s; $P < 0.001$), peak amplitude (control, 15.6 ± 2.1 mV; La^{3+}, 7.8 ± 0.4 mV; $P < 0.01$), and surface area (control, 1,093 ± 142.3 mV·s; La^{3+}, 389 ± 17.1 mV·s; $P < 0.001$; Fig. 8*B*). A specific feature of the La^{3+} action was the abolishment of sporadic subthreshold depolarizations. Note that subthreshold depolarizations in human SP neurons persisted after treatments with TTX (Fig. 2 *A*, *Lower*), synaptic blockers (Fig. 3 *D*, *Right*), or gap junction blockers (Fig. 7*A*, lower traces). These data suggest that La^{3+}-sensitive membrane

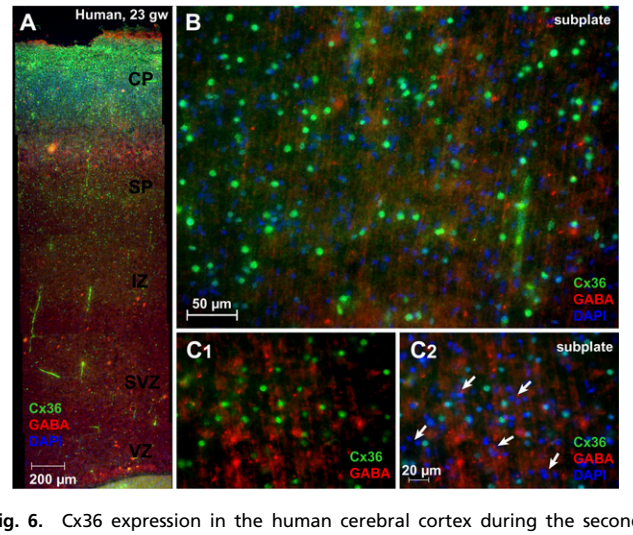

Fig. 6. Cx36 expression in the human cerebral cortex during the second trimester of gestation. (*A*) A composite (mosaic) image acquired at 10x magnification, enveloping the entire cortical wall of a human fetal brain at 23 gw. Cx36-labeled (green) cells were distributed in the intermediate zone (IZ), SP zone, and the CP (GABA, red; DAPI, blue). (*B*) Multiple cells positive for Cx36 (red) in the SP zone. GABA-positive fibers transverse the SP zone in radial direction. (*C1*) SP zone imaged at 20x. (*C2*) Same field as in *C1* with addition of the blue channel (nuclear staining). Arrows mark clusters of Cx36-negative cells in the SP zone.

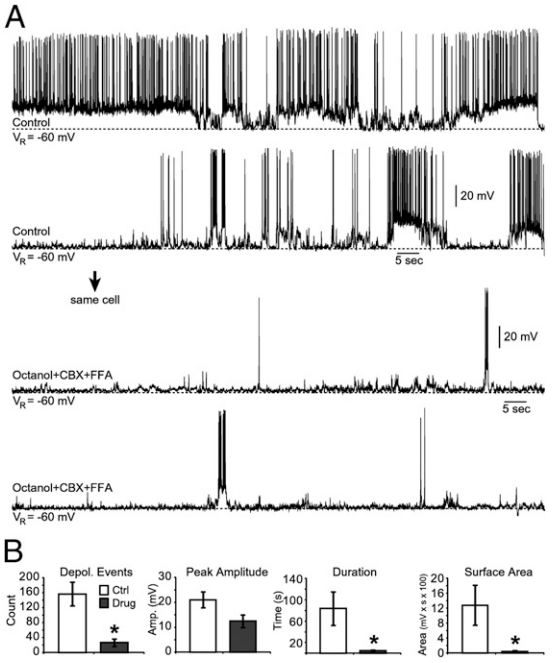

Fig. 7. Cx inhibitors suppress SP neuron activity. (*A*) Recordings of spontaneous electrical activity in control and drug conditions containing (OCT+CBX+FFA) in the same cell ($n = 6$). (*B*) Dynamics of spontaneous electrical activity of human SP neurons before (white) and after (gray) drug application ($n = 6$). *$P < 0.05$.

pores mediate random subthreshold depolarizations in young human neurons during the second trimester of gestation.

To determine whether human SP neurons were coupled via gap junctions 5 mo before birth (at 17–23 gw), we included Lucifer yellow ($n = 16$) or Neurobiotin ($n = 9$) in the intracellular solution that already contained either sulforhodamine 101 or Alexa Fluor 594. Both Lucifer yellow and Neurobiotin have low molecular weights (MWs; 457.8 and 322.8, respectively) allowing them to be transported between electrically coupled cells, whereas sulforhodamine and Alexa Fluor 594 have higher MWs (758.8 and 606.7, respectively) inhibiting their diffusion between cells. We saw no transfer of either Lucifer yellow or Neurobiotin between neurons following ≥25 min of recordings. Alexa Fluor 594 images (or sulforhodamine images) were perfectly correlated with Lucifer yellow images (in separate channels), thus indicating that both dyes remained secluded in the same cell and did not fill neighboring neurons through gap junctions (Fig. 8*C*). Following the peroxidase reaction, Neurobiotin also remained constrained within the injected neuron ($n = 9$), without any signs of dye transfer to the neighboring cells. Immunolabeling of solitary Cx-positive neurons (Figs. 5 *B–F* and 6) and dye transfer experiments (Fig. 8*C*) both suggest that gap junctions are not prominent in human SP neurons at very early stages of cortical development, 5 mo before birth.

Current clamp recordings in human SP neurons held at potentials near −80 mV often showed rapid transitions from resting to depolarized state, and vice versa (Fig. 9*B*). The peak amplitude of subthreshold spontaneous depolarizations was in the range of 15–20 mV (Fig. 9*B*, dashed red line). At less hyperpolarized potentials (approximately −60 mV), such depolarizations brought neurons to the AP threshold (Fig. 9*C*, cell 4). Fast transitions from resting potential to depolarized state and vice versa, combined with consistent peak amplitude in the range of 15–20 mV (Fig. 9 *B* and *C*), suggest that opening of a few membrane pores—or just one membrane pore—is occurring randomly in human SP neurons at this age.

Discussion

The present study investigated spontaneous electrical activity in the human fetal SP zone by using glass electrode recordings from individual neurons. All experiments were performed in acute brain slices with partially preserved synaptic contacts and extracellular matrix (52, 53). We found that spontaneous depolarizations in human SP neurons can occur independently of network activity—AP firing blocked by TTX (Fig. 2). Unprovoked depolarizing potentials were also present when human brain slices were perfused with antagonists of glutamatergic, GABAergic, and glycinergic transmission (Figs. 3 and 4). Pharmacological occlusion of Cx pores, conversely, caused a notable reduction in both the frequency and amplitude of spontaneous depolarizations (Figs. 7 and 8). Several Cx proteins (Cx26, Cx32, and Cx36) were detected in the human fetal cortex at 17–23 gw, by using PCR or immunohistochemistry (Fig. 5, 6). The stimulative effect of low extracellular calcium (Fig. 1 *C–E*), weak effects of TTX and synaptic blockers (Figs. 2–4), the solitary nature of Cx-positive SP cells (Figs. 5 and 6), high sensitivity to La^{3+} (Fig. 8) and the apparent lack of dye coupling (Fig. 8*C*), point to a potential link between Cx hemichannels and early spontaneous activity, which characterizes human SP neurons in the second trimester of gestation (34).

Lowering Extracellular Ca^{2+}. In agreement with the current literature (36, 37, 54), lowering the extracellular Ca^{2+} concentration from 2 mM (experimental) to 1.2 mM (physiological) significantly increased the amount of time SP neurons spent in a depolarized state (Fig. 1). This effect is likely due to a loss of a protective barrier of positively charged divalent cations (55).

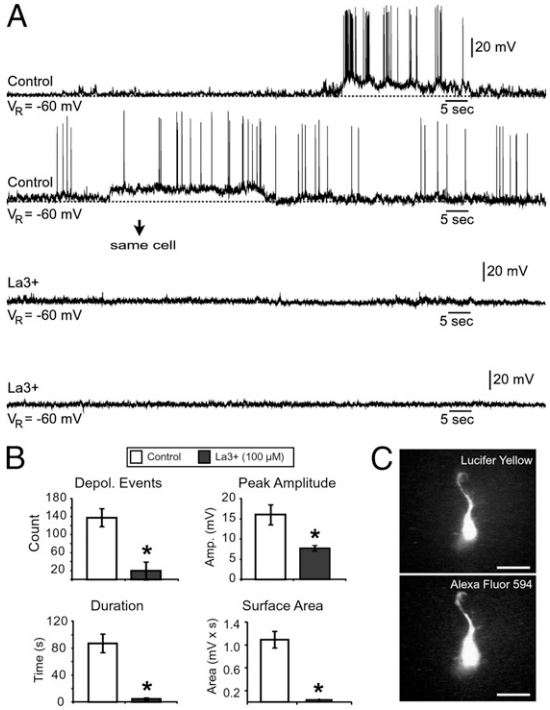

Fig. 8. La^{3+} blocks spontaneous electrical activity in human SP neurons. (*A*) Recordings in human SP neurons before (control) and during application of La^{3+} in the same cell. (*B*) Bath application of La^{3+} significantly reduces the number of depolarizing events, peak amplitude, duration, and surface area. *$P < 0.01$. (*C*) SP neurons were filled with a mixture of dyes containing Lucifer Yellow and Alexa Fluor 594 for 30 min. After the dye injection, the pipette was removed, and images were taken. No evidence of dye coupling was found ($n = 16$). (Scale bars, 10 µm.)

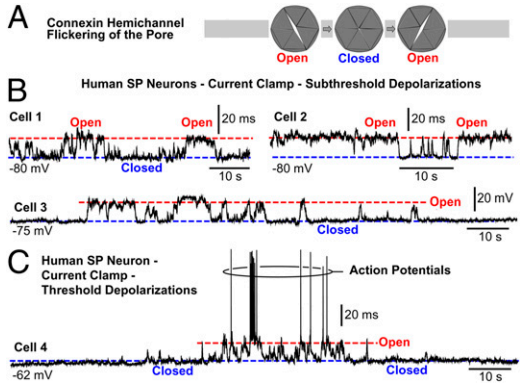

Fig. 9. Spontaneous flickering of Cx pores. (*A*) Schematic drawing of a Cx hemichannel. Neuronal depolarizations occur when the pore is in an open state. (*B*) Current clamp recordings of spontaneous depolarizations in human SP neurons. Cells 1–3 are hyperpolarized with negative holding current, so that AP firing threshold is not reached. (*C*) Current clamp recordings of spontaneous depolarizations in human SP neurons. Cell 4 is closer to the AP firing threshold.

Another possible mechanism involves the basic physiology of hemichannels. Opening of hemichannels is greatly enhanced by lowering the extracellular Ca^{2+} concentration, as demonstrated by single channel recordings (49).

The amount of spontaneous activity observed in our in vitro experiments may be more vigorous than the activity levels actually occurring in vivo. It has been shown that, under physiological conditions, Cx hemichannels can open, but with a lower open probability, whereas under pathological conditions (such as ischemia), Cx hemichannels increase their overall activity (56–58). Therefore, it is possible that the hypoxic conditions imposed on the human fetal brain samples during the harvest and transportation to the laboratory (time period > 3.5 h; *Methods*) may have increased the overall activity of Cx hemichannels.

Classic Synaptic Transmission. In the developing rodent cortex, SP neurons receive glutamatergic, GABAergic, glycinergic, and cholinergic synaptic contacts (32). Histological analysis of human SP neurons has identified the presence of both glutamatergic and GABAergic synaptic contacts during the second trimester of gestation (18, 59). Synaptic stimulations performed in acute brain slices harvested from a postmortem fetal tissue demonstrated the presence of functional synaptic contacts in human SP neurons, although such contacts were rare (34). During the second trimester of gestation (17–23 gw), the human telencephalon is developing in an absence of strong sensory input, consistent with previous experiments examining direct synaptic inputs (34) and experiments based on synaptic blockers (present study). It is also worth emphasizing that thalamocortical and cortico-cortical fibers slowly begin to invade the human SP zone at 24 gw and later (18, 60), and therefore the third trimester of gestation 28–42 wk is a period in human brain development when glutamatergic, GABAergic, and glycinergic synaptic transmission are likely to dominate spontaneous electrical activity and guide the maturation of cortical circuits, as reported in rodents (22). The present study only covered the period between 17 and 23 gw, before a large number of synaptic fibers have invaded the CP, which may explain the weak effects observed in the presence of synaptic blockers (Fig. 3).

Cx Gap Junctions. Cx are the gap junction-forming proteins of vertebrates and are encoded by a multigene family consisting of at least 20 different genes (61). There are several Cx genes expressed in the CNS during development including Cx26, Cx32, and Cx43 (46, 62–64). In rodents, Cx43 is expressed throughout development and is important for neuronal migration (46). Cx26 is specifically expressed during the early stages of development, whereas Cx32 is expressed postnatally in more mature neurons during later stages of development and throughout adulthood (64, 65).

Depending on the human subject and gestational age, in brain sections containing the SP zone, we found mRNA for Cx26 and Cx36, but not Cx43. Antibody staining confirmed the presence of Cx26 protein and the absence of Cx43 in the SP zone. The Cx26 protein was detected along the processes of large cells in SP zone (Fig. 5*F*). In respect to Cx32, there was a discrepancy between the PCR and immunolabeling. We detected multiple cells positive for the Cx32 antibody at 20–22 gw, but failed to detect any Cx32 mRNA expression in samples obtained at 17, 18, 19, and 20 gw (Fig. S3). This discrepancy may be attributed to a difference in gestational age, because Cx32 expression takes place during later stages of development (65). Abundant Cx43 mRNA expression was detected in the GE at 17 gw (Fig. 5*A* and Fig. S3), consistent with an idea that Cx43 plays an important role in tangential migration and maturation of GABAergic neurons, as it does in radial migration of glutamatergic cells (45, 46).

Based on the important role of gap junction coupling in development (46, 62, 66) and the presence of gap junctions among SP neurons in the postnatal rodent cortex (22, 23, 67), we expected to find that human SP neurons during the second trimester of gestation use gap junctions. However, aside from the sensitivity to OCT, CBX, and FFA, which also block hemichannel opening, we did not find any other evidence supporting this notion. More specifically, SP neurons in the human fetal cortex did not show any dye-coupling under the current experimental settings (Fig. 8*C*). In addition, immunohistochemical analysis of Cx labeling revealed that SP neurons have Cx, but they exclusively appear in isolated cells and not in clusters (Figs. 5 and 6). The difference in species (rat vs. human) and difference in developmental stage (postnatal vs. early prenatal) may explain discrepancy between the data obtained in rat after birth (22, 23, 67) and present data obtained in human 5 mo before birth.

Cx Hemichannels. Cx hemichannels are formed by "unpaired" Cx inserted in the plasma membrane, allowing for communication between a cell's cytoplasm and the extracellular space. They are believed to pass ions and molecules smaller than ∼1 kDa (e.g., ATP) during brief channel openings (68, 69). Hemichannel-mediated initiation of spontaneous activity has been reported in both the developing auditory system (70) and rodent ventricular zone (VZ) (71). Factors released through hemichannels from radial glia processes or other sources, such as astrocytes, may be exciting early SP neurons and causing intermittent periods of depolarization (70, 71). Another possibility is that the opening of neuronal hemichannels causes direct depolarizations (Fig. 9*A*). The opening of the Cx hemichannel pore can be purely spontaneous (Fig. 9*A*), or it can be induced by local changes in oxygen, extracellular ions, metabolites, or pH (49, 72–74). Biophysical properties of both Cx hemichannels and SP neurons are compatible with depolarizations observed in whole-cell recordings (Figs. 1–4). More specifically, the Cx hemichannels exhibit large unitary conductances of ∼300 pS (50, 68, 75, 76), whereas young neurons are characterized by a large input resistance (∼1 GΩ) (4, 33, 34). At a resting potential of −60 mV and Cx equilibrium potential of 0 mV, the currents generated by opening of just one Cx pore would cause ∼18 mV depolarization in SP neurons. Current clamp recordings in human SP neurons often showed rapid transitions from resting to depolarized state (Fig. 9*B*, dashed red line). Fast transitions from resting potential to depolarized state and vice versa, combined with consistent peak amplitude in the range of 15–20 mV (Fig. 9 *B* and *C*), are consistent with the idea that opening of a few hemichannels—or

just one hemichannel—may exert large impacts on the cellular physiology, as previously shown in melanotrophs (77).

Plausible Mechanism. Four lines of reasoning suggest that the spontaneous opening (flickering) of Cx hemichannels is a plausible mechanism for the generation of spontaneous activity. (*i*) Within the first two trimesters of gestation, before thalamocortical fibers invade the CP, functional synaptic contacts are scarce (34). Flickering of Cx hemichannels does not require functional synaptic contacts or operating neuronal networks. (*ii*) At this early stage in human cortical development, electrical activity is not used for information processing, but rather for driving gene expression, neuronal migration, maturation, and synapse formation. Young postmitotic neurons require occasional bursts of AP firing just to maintain their intracellular reactions, to mark their presence in the new location, and to attract and keep synaptic contacts. This activity can be completely random, as the observed depolarizations in human SP neurons were completely random (Figs. 1–4 and 9). (*iii*) Spontaneous flickering of membrane pores is energetically favorable for the cell—it does not require significant energy from the host cell or any other cell in the neighborhood. (*iv*) In utero fluctuations of gases, metabolites, and ions may increase the frequency of Cx hemichannel openings (73, 74), thus suggesting that normal physiological processes, including physical activity in pregnant mothers, may stimulate fetal electrical activity and fetal brain development.*

Health Relevance. The present study demonstrates that spontaneous electrical activity in the human SP zone at midgestation is not exclusively driven by a network of electrically and synaptically coupled neurons, but instead is strongly influenced by Cx pores that are present in the fetal cerebral cortex (Figs. 5 and 6). Closing of the Cx hemichannels by La^{3+} (a putative hemichannel antagonist) or by a plethora of gap junction antagonists invariably resulted in silencing of human fetal SP neurons (Figs. 7 and 8). It seems that Cx-based hemichannels support sustained depolarized episodes (UP states) in developing human cortex 5 mo before birth. Given the importance of spontaneous bioelectric activity for healthy brain development (4–6, 8, 44), and the vulnerability of human cortex in the first and second trimester of gestation, it is important to address a possibility that contamination of food, water, and mother's skin with La^{3+}, Gd^{3+}, OCT, lindane, fenamates, 18-α-glycyrrhetinic acid, and similar agents that interfere with Cx channel opening may result in a prenatal brain injury.

Methods

Human Tissue. Human fetal brain tissue (n = 12 cases), within the second trimester of gestation (Table 1), was obtained from the Tissue Repository of the Albert Einstein College of Medicine (Bronx, NY) within 3.5 h postmortem. Tissue fragments were examined only with proper parental consent and the approval of the Ethics Committees at the Albert Einstein College of Medicine and the University of Connecticut. No apparent abnormalities that could influence the development of the CNS were noticed at the time of tissue collection. Fetal age was estimated on the basis of weeks after ovulation, crown–rump length, and anatomical landmarks. Apart from gestational age and sex, no other information was received. Tissue specimens were transferred on ice in Hanks' balanced salt solution with 0.75% antibiotic/antimycotic (Sigma) and oxygenated with a portable 5% CO_2/95% O_2 tank from the Bronx to Farmington, CT (travel time was ∼3.5 h).

Whole-Cell Patch-Clamp Recordings. All physiological recordings were performed on the day of tissue collection. Brain slices, 500-μm to 1-mm thick, obtained from the medial telencephalic wall of the occipital lobe, were sectioned by free hand while kept on ice-cold ACSF solution (53). The ACSF contained (in mM) 125 NaCl, 2.3 KCl, 26 $NaHCO_3$, 2 $MgSO_4$, 1.26 KH_2PO_4, 2 $CaCl_2$, and 10 glucose (pH 7.3; osmolality = 310 mOsm/kg). Slices were incubated at 37 °C for 30 min and then stored at room temperature before recordings. Patch-clamp recordings were performed as described (33, 34). Briefly, acute brain slices were transferred to an Olympus BX51WI upright microscope and gravity perfused with aerated (5% CO_2/95% O_2) ACSF at 32 °C. Individual cells in the SP were selected by using infrared differential interference contrast video microscopy (Fig. 1 *A1* and *A2*). Patch pipettes (7–10 MΩ) were filled with an intracellular solution containing (in mM) 135 K gluconate, 10 Hepes, 2 $MgCl_2$, 3 ATP-Na_2, 0.3 GTP-Na_2, 0.5 EGTA and 10 phosphocreatine Na_2 (pH 7.3 adjusted with KOH, osmolality = 300 mOsm/kg). To reveal cellular morphology under the epifluorescence microscopy, either sulforhodamine 101, Alexa Fluor 594 (Molecular Probes), Lucifer Yellow 457 (Sigma), or Neurobiotin (Vector Labs) was added to the patch pipette at concentrations between 30 and 50 μM (Fig. 1 *A2* and *B*). Membrane potential values were corrected for liquid junction potentials as follows: −10.4 mV. Whole-cell patch-clamp recordings and voltage and current clamp configuration were used to determine the basic electrophysiological properties of each individual cell. For voltage clamp recordings, SP neurons were held at −70 mV. The voltages were then stepped from −90 to +90 mV (step 10 mV), for a duration of 50 ms, to determine the presence of voltage-gated transmembrane currents. Cells were then switched to current clamp configuration to determine the resting membrane potential. To determine whether selected cells were able to fire repetitive APs, the membrane potential was held at −60 mV by injecting DC negative current (range from −3 to −22 pA). A series of current steps (−20 to +70 pA in 5- or 10-pA steps) were then applied to the cell for a duration of 350 ms (Fig. 1 *A*, *Inset*).

Recordings of Spontaneous Activity. Upon verification of repetitive AP firing (Fig. 1 *C*, *Inset*), we proceeded to record spontaneous electrical activity (Fig. 1 *C*, *Upper*). Voltage monitoring was performed in current clamp with bias DC current (from −3 to −22 pA) to clamp the neuron at approximately −60 mV. Once the recording started, the intensity of bias current was not changed. Spontaneous activity was continuously monitored for a minimum of 5 min before drug application (Control). A cell was identified as being spontaneously active, based on periods of depolarization (amplitude > 5 mV, duration >25 ms) either with or without AP firing. Following control measurements (5 min), the recording of same duration (5 min) was carried out in the presence of drugs. All substances were purchased from Sigma and bath perfused at an average rate of 2–3 mL/min. Stock solutions were prepared as follows: TTX and La^{3+} in H_2O; FFA, CBX, and bicuculline in ethanol and H_2O; APV in H_2O and NaOH, strychnine and DNQX in DMSO. Stock solutions were stored at −20 °C and diluted in ACSF on the day of the experiment. Because La^{3+} precipitates in normal ACSF, we used a modified Krebs–Ringers solution (49) in both control recordings and in the presence of La^{3+}. The Krebs–Ringers solution contained (in mM) 140 NaCl, 5.4 KCl, 1 $MgCl_2$, 1.2 $CaCl_2$, 10 mM Hepes, pH 7.4. Syn. Block + TTX refers to a mixture of drugs including 20 μM DNQX, 20 μM APV, 20 μM bicuculline, 20 μM strychnine, and 1 μM TTX.

Data Analysis. Data analysis was performed offline in Clampfit (Version 9.2), Excel (Microsoft), and SigmaStat (Version 3.2). Summary data are expressed as mean ± SEM. If the data passed the normality test, we used a paired Student t test. If the normality test failed, the statistical difference between measures was based on a Mann–Whitney test. Results were considered statistically significant if $P \leq 0.05$.

Voltage dwelling. An all-points histogram is often used in cellular electrophysiology to quantify spontaneous activity and detect UP and DOWN states (3, 78). This method plots the frequency of occurrence of various values of membrane potential for every point in a digitized record. An all-points histogram was made for each cell in the present study by using Clampfit (Version 9.2). In the offline analysis, the resting membrane potential of all neurons was set to 0 mV (Clampfit Version 9.2, Adjust baseline). From there, we counted the number of digitized samples spent at each membrane potential with a set bin of 1 mV. The number of samples can be converted to time by multiplying by the sampling interval (100 μs) by the total number of samples in the voltage bin. For all-points histograms, deviation from resting membrane potential is plotted on the X axis, and dwelling time on the Y axis by using a semilogarithmic scale [$\log_{(10)}$]. The peak of the histogram contour (Fig. 1*D*) stands at 0 mV (adjusted resting potential), meaning that the majority of time during the 5-min recording session was spent at the resting membrane potential.

Quantification of spontaneous activity. Quantification of spontaneous activity, including the number of events, average peak amplitude, event duration, instantaneous frequency, and interevent interval, was performed in Clampfit (Version 9.2) by using the Event Threshold function. For each neuron, and

*Labonte-Lemoyne E, Curnier D, Ellemberg D, Society for Neuroscience Annual Meeting, November 9–13, 2013, San Diego, poster 217.08.

each experimental condition (e.g., control and drug), a minimum of 5 min of spontaneous activity was recorded. Spontaneous events were defined as those in which the membrane potential crossed a set threshold (5 mV above resting). Setting thresholds >5 mV allowed us to focus primarily on large and sustained depolarizing events (UP states) of SP neurons, as opposed to small and fast electrical transients mixed with noise. Spontaneous events were defined as those in which the membrane potential crossed a set threshold of 5 mV above rest and a duration >25 ms. Event amplitude was defined by the maximum peak change (millivolt, mV) of the event from baseline (0 mV). Event duration was measured as the amount of time spent above the threshold value. Interevent intervals were defined as time that passes between the onsets of two subsequent events.

PCR. Two fetal brains were used for PCR ($n = 2$ cases; 17 and 19 gw). In the first specimen (19 gw), the cortical slices were microdissected into two halves. The pial half was termed CP; the ventricular half was termed SVZ. In the second specimen (17 gw), microdissection was not performed; hence, all cortical zones were homogenized together, and here termed "cortical mantle" (CM). Both medial and lateral GEs were included in the sample marked "GE." Total human brain (hBr) RNA from an 18-y-old male was purchased from Clontech. RNA for all fetal samples was purified by using TRIzol according to the manufacturer's instructions. cDNA was made from 500 ng of RNA from each sample with both 0.94 μM oligo(dT)20 and 4 μM random hexamer primers in the reaction. GE cDNA was made with SuperScriptIII reverse transcriptase (Invitrogen) according the manufacturer's instructions. cDNA for all other samples was made with M-MuLV (New England Biolabs) according to the manufacturer's instructions. Primer sequences are listed in Fig. S3. PCR was performed with GoTaq polymerase (Promega) by using the following conditions: 94 °C, 4 min; 94 °C, 30 s; 55 °C, 30 s; 72 °C, 30 s; 72 °C, 10 min for 36 cycles, except for β-Actin (28 cycles), Cx26 (32 cycles), Cx32 variant 2 (33 cycles), and Cx43 (35 cycles). PCR products were visualized on ethidium bromide-stained gels.

Immunohistochemistry and Imaging. After electrophysiological recordings, brain slices were fixed in 4% (wt/vol) paraformaldehyde (PFA) for 30 min, embedded in Tissue-Tec OCT mounting medium, and resectioned on a microtome to 20-μm-thick sections ($n = 4$ cases, 20 gw; $n = 1$ case, 21 gw; $n = 1$ case, 22 gw). Sections were mounted onto gelatin-coated glass coverslips, permeabilized, and blocked with normal goat serum in 0.3% Triton X-100. Antibodies for Cx32, Cx26, and Cx43 were purchased from Invitrogen, Connexin 36/GJA9 antibody (5A5), Novus Biologicals USA, and βIII-tubulin from Sigma. Primary antibodies were applied overnight (4 °C) at the following concentrations: Cx32 rabbit polyclonal and mouse monoclonal (1:100), Cx26 rabbit polyclonal (1:100), Cx43 rabbit polyclonal and mouse monoclonal (1:100), and βIII-tubulin (1:500). Sections were rinsed 3 × 8 min in phosphate buffer (PB) with normal goat serum, and secondary antibodies were applied at room temperature for 1 h. Alexa Fluor 488 anti-rabbit, Alexa Fluor 594 anti-rabbit, Alexa Fluor 594 anti-mouse, and Alexa 488 anti-mouse conjugated secondary antibodies were purchased from Invitrogen. Sections were rinsed 3 × 10 min with PB and coverslipped with glycerol and p-phenylenediamine (Sigma). For Neurobiotin staining, brain slices were removed from the recording chamber at the end of the recording session and fixed in 4% PFA for 24 h at 4 °C. The next day, fixed slices were rinsed and incubated for 2 h with 3% H_2O_2 in PB to inhibit endogenous peroxidases. Slices were incubated overnight with an avidin–biotin reaction (ABC kit; Vectorlab) at 4 °C. Following overnight incubation, slices were warmed to room temperature and then rinsed 4 × 8 min in PB followed by a 3,3′-diaminobenzidine reaction. The reaction was intensified with 0.03% H_2O_2. Slices were washed, mounted, dehydrated with xylenes, and coverslipped with Permount. Neurobiotin-stained neurons were analyzed by using an Axiovert microscope (Zeiss).

ACKNOWLEDGMENTS. We thank Klaus Ballanyi for discussions on the physiological concentrations of extracellular calcium; Douglas Oliver and Deborah Bishop for help with apotome imaging; and Nevena Radonjic and Nicole Glidden for help with immunostaining and RNA extraction. This work was supported by National Institutes of Health (NIH) Training Grant 5T32NS041224 (to A.R.M.), NIH R01 Grant (to N.Z.), and an institutional Health Center Research Advisory Council grant (to S.D.A.). Human fetal tissue was obtained from B. Poulos at the Albert Einstein College of Medicine, Tissue Repository.

1. Timofeev I, Grenier F, Bazhenov M, Sejnowski TJ, Steriade M (2000) Origin of slow cortical oscillations in deafferented cortical slabs. *Cereb Cortex* 10(12):1185–1199.
2. Bi G, Poo M (2001) Synaptic modification by correlated activity: Hebb's postulate revisited. *Annu Rev Neurosci* 24:139–166.
3. Wilson CJ (2008) *Up and down states, Scholarpedia* **3**, 1410, revision #91903.
4. Moody WJ, Bosma MM (2005) Ion channel development, spontaneous activity, and activity-dependent development in nerve and muscle cells. *Physiol Rev* 85(3):883–941.
5. Corner MA (2008) Spontaneous neuronal burst discharges as dependent and independent variables in the maturation of cerebral cortex tissue cultured in vitro: A review of activity-dependent studies in live 'model' systems for the development of intrinsically generated bioelectric slow-wave sleep patterns. *Brain Res Brain Res Rev* 59(1):221–244.
6. Spitzer NC (2002) Activity-dependent neuronal differentiation prior to synapse formation: The functions of calcium transients. *J Physiol Paris* 96(1–2):73–80.
7. Khazipov R, Luhmann HJ (2006) Early patterns of electrical activity in the developing cerebral cortex of humans and rodents. *Trends Neurosci* 29(7):414–418.
8. Katz LC, Shatz CJ (1996) Synaptic activity and the construction of cortical circuits. *Science* 274(5290):1133–1138.
9. Mohajerani MH, Cherubini E (2006) Role of giant depolarizing potentials in shaping synaptic currents in the developing hippocampus. *Crit Rev Neurobiol* 18(1–2):13–23.
10. Greer JJ, Funk GD, Ballanyi K (2006) Preparing for the first breath: Prenatal maturation of respiratory neural control. *J Physiol* 570(Pt 3):437–444.
11. McCabe AK, Chisholm SL, Picken-Bahrey HL, Moody WJ (2006) The self-regulating nature of spontaneous synchronized activity in developing mouse cortical neurones. *J Physiol* 577(Pt 1):155–167.
12. Turrigiano G (2012) Homeostatic synaptic plasticity: Local and global mechanisms for stabilizing neuronal function. *Cold Spring Harb Perspect Biol* 4(1):a005736.
13. Voigt T, Opitz T, de Lima AD (2001) Synchronous oscillatory activity in immature cortical network is driven by GABAergic preplate neurons. *J Neurosci* 21(22):8895–8905.
14. Kanold PO, Luhmann HJ (2010) The subplate and early cortical circuits. *Annu Rev Neurosci* 33:23–48.
15. Ghosh A, Antonini A, McConnell SK, Shatz CJ (1990) Requirement for subplate neurons in the formation of thalamocortical connections. *Nature* 347(6289):179–181.
16. Kanold PO, Kara P, Reid RC, Shatz CJ (2003) Role of subplate neurons in functional maturation of visual cortical columns. *Science* 301(5632):521–525.
17. Kanold PO (2004) Transient microcircuits formed by subplate neurons and their role in functional development of thalamocortical connections. *Neuroreport* 15(14):2149–2153.
18. Kostovic I, Rakic P (1990) Developmental history of the transient subplate zone in the visual and somatosensory cortex of the macaque monkey and human brain. *J Comp Neurol* 297(3):441–470.
19. Friauf E, McConnell SK, Shatz CJ (1990) Functional synaptic circuits in the subplate during fetal and early postnatal development of cat visual cortex. *J Neurosci* 10(8):2601–2613.
20. Hanganu IL, Kilb W, Luhmann HJ (2002) Functional synaptic projections onto subplate neurons in neonatal rat somatosensory cortex. *J Neurosci* 22(16):7165–7176.
21. Higashi S, Molnár Z, Kurotani T, Toyama K (2002) Prenatal development of neural excitation in rat thalamocortical projections studied by optical recording. *Neuroscience* 115(4):1231–1246.
22. Dupont E, Hanganu IL, Kilb W, Hirsch S, Luhmann HJ (2006) Rapid developmental switch in the mechanisms driving early cortical columnar networks. *Nature* 439(7072):79–83.
23. Hanganu IL, Okabe A, Lessmann V, Luhmann HJ (2009) Cellular mechanisms of subplate-driven and cholinergic input-dependent network activity in the neonatal rat somatosensory cortex. *Cereb Cortex* 19(1):89–105.
24. Calarco CA, Robertson RT (1995) Development of basal forebrain projections to visual cortex: DiI studies in rat. *J Comp Neurol* 354(4):608–626.
25. Mechawar N, Cozzari C, Descarries L (2000) Cholinergic innervation in adult rat cerebral cortex: A quantitative immunocytochemical description. *J Comp Neurol* 428(2):305–318.
26. Volpe JJ (2000) Overview: Normal and abnormal human brain development. *Ment Retard Dev Disabil Res Rev* 6(1):1–5.
27. McQuillen PS, Ferriero DM (2005) Perinatal subplate neuron injury: Implications for cortical development and plasticity. *Brain Pathol* 15(3):250–260.
28. Rice D, Barone S, Jr (2000) Critical periods of vulnerability for the developing nervous system: Evidence from humans and animal models. *Environ Health Perspect* 108(Suppl 3):511–533.
29. Zecević N (1993) Cellular composition of the telencephalic wall in human embryos. *Early Hum Dev* 32(2-3):131–149.
30. Bystron I, Blakemore C, Rakic P (2008) Development of the human cerebral cortex: Boulder Committee revisited. *Nat Rev Neurosci* 9(2):110–122.
31. Marder E (2011) Variability, compensation, and modulation in neurons and circuits. *Proc Natl Acad Sci USA* 108(Suppl 3):15542–15548.
32. Luhmann HJ, Kilb W, Hanganu-Opatz IL (2009) Subplate cells: Amplifiers of neuronal activity in the developing cerebral cortex. *Front Neuroanat* 3:19.
33. Moore AR, et al. (2009) Electrical excitability of early neurons in the human cerebral cortex during the second trimester of gestation. *Cereb Cortex* 19(8):1795–1805.
34. Moore AR, Zhou WL, Jakovcevski I, Zecevic N, Antic SD (2011) Spontaneous electrical activity in the human fetal cortex in vitro. *J Neurosci* 31(7):2391–2398.
35. André M, et al. (2010) Electroencephalography in premature and full-term infants. Developmental features and glossary. *Neurophysiol Clin* 40(2):59–124.
36. Brumberg JC, Nowak LG, McCormick DA (2000) Ionic mechanisms underlying repetitive high-frequency burst firing in supragranular cortical neurons. *J Neurosci* 20(13):4829–4843.

37. Ruangkittisakul A, Secchia L, Bornes TD, Palathinkal DM, Ballanyi K (2007) Dependence on extracellular Ca2+/K+ antagonism of inspiratory centre rhythms in slices and en bloc preparations of newborn rat brainstem. *J Physiol* 584(Pt 2):489–508.
38. Weliky M, Katz LC (1999) Correlational structure of spontaneous neuronal activity in the developing lateral geniculate nucleus in vivo. *Science* 285(5427):599–604.
39. Garaschuk O, Linn J, Eilers J, Konnerth A (2000) Large-scale oscillatory calcium waves in the immature cortex. *Nat Neurosci* 3(5):452–459.
40. Xu H, Whelan PJ, Wenner P (2005) Development of an inhibitory interneuronal circuit in the embryonic spinal cord. *J Neurophysiol* 93(5):2922–2933.
41. Hanganu IL, Ben-Ari Y, Khazipov R (2006) Retinal waves trigger spindle bursts in the neonatal rat visual cortex. *J Neurosci* 26(25):6728–6736.
42. Allène C, et al. (2008) Sequential generation of two distinct synapse-driven network patterns in developing neocortex. *J Neurosci* 28(48):12851–12863.
43. Momose-Sato Y, Nakamori T, Sato K (2012) Pharmacological mechanisms underlying switching from the large-scale depolarization wave to segregated activity in the mouse central nervous system. *Eur J Neurosci* 35(8):1242–1252.
44. Blankenship AG, Feller MB (2010) Mechanisms underlying spontaneous patterned activity in developing neural circuits. *Nat Rev Neurosci* 11(1):18–29.
45. Liu X, Sun L, Torii M, Rakic P (2012) Connexin 43 controls the multipolar phase of neuronal migration to the cerebral cortex. *Proc Natl Acad Sci USA* 109(21):8280–8285.
46. Elias LA, Turmaine M, Parnavelas JG, Kriegstein AR (2010) Connexin 43 mediates the tangential to radial migratory switch in ventrally derived cortical interneurons. *J Neurosci* 30(20):7072–7077.
47. Yuste R, Peinado A, Katz LC (1992) Neuronal domains in developing neocortex. *Science* 257(5070):665–669.
48. Cruikshank SJ, Landisman CE, Mancilla JG, Connors BW (2005) Connexon connexions in the thalamocortical system. *Prog Brain Res* 149:41–57.
49. Contreras JE, et al. (2002) Metabolic inhibition induces opening of unapposed connexin 43 gap junction hemichannels and reduces gap junctional communication in cortical astrocytes in culture. *Proc Natl Acad Sci USA* 99(1):495–500.
50. Retamal MA, et al. (2007) Cx43 hemichannels and gap junction channels in astrocytes are regulated oppositely by proinflammatory cytokines released from activated microglia. *J Neurosci* 27(50):13781–13792.
51. Brokamp C, Todd J, Montemagno C, Wendell D (2012) Electrophysiology of single and aggregate Cx43 hemichannels. *PLoS ONE* 7(10):e47775.
52. Edwards FA, Konnerth A, Sakmann B, Takahashi T (1989) A thin slice preparation for patch clamp recordings from neurones of the mammalian central nervous system. *Pflugers Arch* 414(5):600–612.
53. Moore AR, Zhou WL, Jakovcevski I, Zecevic N, Antic SD (2012) *Isolated Central Nervous System Circuits*, ed Ballanyi K (Springer, Secaucus, NJ), Vol 73, pp 125–158.
54. Sheroziya MG, von Bohlen Und Halbach O, Unsicker K, Egorov AV (2009) Spontaneous bursting activity in the developing entorhinal cortex. *J Neurosci* 29(39):12131–12144.
55. Frankenhaeuser B, Hodgkin AL (1957) The action of calcium on the electrical properties of squid axons. *J Physiol* 137(2):218–244.
56. John SA, Kondo R, Wang SY, Goldhaber JI, Weiss JN (1999) Connexin-43 hemichannels opened by metabolic inhibition. *J Biol Chem* 274(1):236–240.
57. Thompson RJ, Zhou N, MacVicar BA (2006) Ischemia opens neuronal gap junction hemichannels. *Science* 312(5775):924–927.
58. Bennett MV, et al. (2012) Connexin and pannexin hemichannels in inflammatory responses of glia and neurons. *Brain Res* 1487:3–15.
59. Kostovic I, Rakic P (1980) Cytology and time of origin of interstitial neurons in the white matter in infant and adult human and monkey telencephalon. *J Neurocytol* 9(2):219–242.
60. Kostović I, Judas M (2010) The development of the subplate and thalamocortical connections in the human foetal brain. *Acta Paediatr* 99(8):1119–1127.
61. Willecke K, et al. (2002) Structural and functional diversity of connexin genes in the mouse and human genome. *Biol Chem* 383(5):725–737.
62. Nadarajah B, Jones AM, Evans WH, Parnavelas JG (1997) Differential expression of connexins during neocortical development and neuronal circuit formation. *J Neurosci* 17(9):3096–3111.
63. Momose-Sato Y, Honda Y, Sasaki H, Sato K (2005) Optical imaging of large-scale correlated wave activity in the developing rat CNS. *J Neurophysiol* 94(2):1606–1622.
64. Cina C, Bechberger JF, Ozog MA, Naus CC (2007) Expression of connexins in embryonic mouse neocortical development. *J Comp Neurol* 504(3):298–313.
65. Dermietzel R, et al. (1989) Differential expression of three gap junction proteins in developing and mature brain tissues. *Proc Natl Acad Sci USA* 86(24):10148–10152.
66. Bittman K, Owens DF, Kriegstein AR, LoTurco JJ (1997) Cell coupling and uncoupling in the ventricular zone of developing neocortex. *J Neurosci* 17(18):7037–7044.
67. Sun JJ, Luhmann HJ (2007) Spatio-temporal dynamics of oscillatory network activity in the neonatal mouse cerebral cortex. *Eur J Neurosci* 26(7):1995–2004.
68. Bennett MV, Contreras JE, Bukauskas FF, Sáez JC (2003) New roles for astrocytes: Gap junction hemichannels have something to communicate. *Trends Neurosci* 26(11): 610–617.
69. Goodenough DA, Paul DL (2003) Beyond the gap: Functions of unpaired connexon channels. *Nat Rev Mol Cell Biol* 4(4):285–294.
70. Tritsch NX, Yi E, Gale JE, Glowatzki E, Bergles DE (2007) The origin of spontaneous activity in the developing auditory system. *Nature* 450(7166):50–55.
71. Weissman TA, Riquelme PA, Ivic L, Flint AC, Kriegstein AR (2004) Calcium waves propagate through radial glial cells and modulate proliferation in the developing neocortex. *Neuron* 43(5):647–661.
72. Pfahnl A, Dahl G (1999) Gating of cx46 gap junction hemichannels by calcium and voltage. *Pflugers Arch* 437(3):345–353.
73. Evans WH, De Vuyst E, Leybaert L (2006) The gap junction cellular internet: Connexin hemichannels enter the signalling limelight. *Biochem J* 397(1):1–14.
74. Retamal MA (2014) Connexin and Pannexin hemichannels are regulated by redox potential. *Front Physiol* 5:80.
75. Wang N, et al. (2012) Connexin mimetic peptides inhibit Cx43 hemichannel opening triggered by voltage and intracellular Ca2+ elevation. *Basic Res Cardiol* 107(6):304.
76. González D, Gómez-Hernández JM, Barrio LC (2006) Species specificity of mammalian connexin-26 to form open voltage-gated hemichannels. *FASEB J* 20(13):2329–2338.
77. Kehl SJ, McBurney RN (1989) The firing patterns of rat melanotrophs recorded using the patch clamp technique. *Neuroscience* 33(3):579–586.
78. Cowan RL, Wilson CJ (1994) Spontaneous firing patterns and axonal projections of single corticostriatal neurons in the rat medial agranular cortex. *J Neurophysiol* 71(1): 17–32.